arXiv:astro-ph/9705030v2 13 May 1997

Chemical Abundances of Planetary Nebulae in the Sagittarius Dwarf Elliptical Galaxy [1]

J. R. Walsh

Space Telescope European Co-ordinating Facility, European Southern Observatory, Karl-Schwarzschild Strasse 2, D-85748 Garching bei München, Germany

and

G. Dudziak

European Southern Observatory, Karl-Schwarzschild Strasse 2, D-85748 Garching bei München, Germany

and

D. Minniti

Lawrence Livermore National Laboratory, MS L-413, P.O Box 808, Livermore, CA 94550

and

A. A. Zijlstra

European Southern Observatory, Karl-Schwarzschild Strasse 2, D-85748 Garching bei München, Germany

ABSTRACT

Spectrophotometry and imaging of the two planetary nebulae He 2-436 and Wray 16-423, recently discovered to be in the Sagittarius dwarf elliptical galaxy, are presented. Wray 16-423 is a high excitation planetary nebula (PN) with a hot central star. In contrast He 2-436 is a high density nebula with a cooler central star and evidence of local dust, the extinction exceeding that for Wray 16-423 by E_{B-V} = 0.28. The extinction to Wray 16-423, (E_{B-V}=0.14) is consistent with the line of sight extinction to the Sagittarius Dwarf. Both PN show Wolf-Rayet features in their spectra, although the lines are weak in Wray 16-423. Images in [O III] and Hα+[N II], although affected by poor seeing, yield a diameter of 1.2″ for Wray 16-423 after deconvolution, whilst He 2-436 was unresolved. He 2-436 has a luminosity about twice that of Wray 16-423

---

[1] Based on observations at the European Southern Observatory, La Silla

and its size and high density suggest a younger nebula. In order to reconcile the differing luminosity and nebular properties of the two nebulae with similar age progenitor stars, it is suggested that they are on He burning tracks

An abundance analysis is presented for both PN using empirical abundance determinations. The abundance pattern is very similar in both nebulae and both show an oxygen depletion of -0.4 dex with respect to the mean oxygen abundance of Galactic planetary nebulae and $[O/H] = -0.6$. The Sagittarius PN progenitor stars are representative of the higher metallicity tail of the Sagittarius population. The pattern of abundance depletion is similar to that in the only other planetary nebula in a dwarf galaxy companion of the Milky Way, that in Fornax, for which new spectra are presented. However the abundances are larger than for Galactic halo PN suggesting a later formation age. The oxygen abundance of the Sagittarius galaxy deduced from its PN, shows similarities with that of dwarf ellipticals around M 31, advancing the notion that this galaxy was a dwarf elliptical before its interaction with the Milky Way.

Subject headings: Planetary Nebulae: individual – He 2-436 and Wray 16-423; Galaxies: individual – Sagittarius; Galaxies: individual – Fornax; Dwarf elliptical galaxies

1. Introduction

The Sagittarius dwarf elliptical galaxy (synonymous with the Sagittarius dwarf spheroidal) was discovered only in 1994 by Ibata et al. (1994, 1995) and lies in a region some ten degrees from the Galactic Centre, at a distance of 25 ± 3 kpc. Extensive photometry and star counts have shown that the full extent of this galaxy is larger than first revealed. Alard (1996) and Alcock et al. (1997) found RR Lyrae stars belonging to this galaxy in fields out to Galactic latitude $b = -2°$ and Mateo et al. (1996) and Ibata et al. (1997) found members extending below $b = -25°$, implying an extension of at least 25°, or more than 10 kpc for a distance of 25 kpc. The galaxy appears to be prolate with an axis ratio of 3:1 (Ibata et al. 1997). Based on determination of its orbit, the galaxy must have undergone many orbital crossing of the Galaxy, but although distorted has not been disrupted (Ibata et al. 1997; Mateo et al. 1996). There are four globular clusters associated with the Sagittarius dwarf, of which M 54 may constitute the nucleus (Ibata et al. 1994; da Costa & Armandroff 1995; Minniti et al. 1996). The galaxy appears to be more massive than the majority of Galactic dwarf ellipticals and its luminosity is $\geq 2\times10^7$ $L_\odot$ (Mateo et al. 1996). Zijlstra & Walsh (1996) during the course of a survey of the dynamics of planetary nebulae (PN) toward the Galactic Bulge discovered that two previously catalogued (Galactic) PN in the direction towards the Sagittarius dwarf had radial velocities in agreement with that of the tidal tail of the Sagittarius galaxy. Figure 1 in Zijlstra & Walsh (1996) shows the position of these two PN (He 2-436, (Henize 1967) and Wray 16-423 (Wray 1966)) in relation to the galaxy and its globular clusters. A third PN (PRMG-1) also lies in the direction towards this galaxy ($l = 6.0, b = -41.9$), and has been considered as a halo planetary nebula on the basis of its low abundances (Pẽna et al. 1989). PRMG-1 clearly does not belong to the Galactic bulge population so could be a possible member of the Sagittarius dwarf; lacking a radial velocity measurement however, its membership is unproven.

In view of the importance of these PN for studying the stellar population and star formation history of the closest dwarf galaxy to our Galaxy, narrow and broad slit spectrophotometry and emission line imagery were obtained of both He 2-436 and Wray 16-423 in order to study their chemical abundances and their size and structure. In addition, spectroscopy of the only other PN known in a dwarf elliptical satellite galaxy of the Milky Way, that in Fornax (Danziger et al. 1978), was also obtained. Section 2 presents the observations and reductions and Section 3 the analysis. Section 4 discusses the abundance pattern revealed by these three nebulae in the context of the chemical evolution of the local dwarf galaxies.

2. Observations and Reductions

2.1. Spectrometry

Long slit observations of both Sagittarius dwarf galaxy PN were obtained with the ESO NTT and Nasmyth imager/spectrograph EMMI using the Red Imaging and Low Dispersion Mode (RILD) mode, with grism #3 and a slit width of 1.5″. The RILD mode allows imaging, long-slit grism spectroscopy, slitless and multi-object spectroscopy over the wavelength range 4000 - 10000Å. The detector was a Tek 2048×2048 thinned chip (ESO#36, TK512CB) with 24μm pixels (0.27″) and the spectral resolution (2 pixels) was 4.5Å. Details of the observations are listed in Table 1. He-Ar comparison lamp spectra and broad slit (5.0″) exposures of the spectrophotometric standard EG274 (Hamuy et al. 1994) were obtained for wavelength and flux calibration respectively.

Both Sagittarius PN were also observed with the ESO 1.52m telescope and Boller and Chivens spectrograph with a Loral/Lesser 2048^2 CCD (ESO #39) as detector (15μm pixels and read-out noise 5e$^-$). Low dispersion spectra (131Å/mm) covering the optical range at a resolution of 5Å (up to 7Å in the blue) were obtained with both short and long exposures to record bright emission lines unsaturated as well as weak lines. Broad slit spectra were also obtained of Wray 16-423 for determination of the absolute line flux. Higher dispersion spectra with a holographic grating (#32) giving a resolution of 0.99Å were used to resolve the density sensitive [O II] 3627,3729Å doublet, and optimally record the weak C II 4267Å line. All details are given in Table 1. Broad slit observations of LTT 3864 (Hamuy et al. 1994) accompanied all the PN observations for flux calibration. For the low dispersion spectra, the very high quantum efficiency in the blue for this coated CCD meant that there was significant contamination of the spectra from second order light at wavelengths above 6300Å, despite using a GG345 blocking filter. As a result the sensitivity curves derived from the spectrophotometric standard star spectra are not reliable in the red (>6500Å) despite using a standard star of late spectral type. Exposures of a He-Ar lamp were used for the purposes of wavelength calibration. The seeing was around 1-1.5″ for the 1.5m observations and the observing nights photometric except the last when the higher dispersion spectra were obtained.

All the 2-D spectra were reduced in the usual way, using the spectroscopic packages in IRAF[2]. The bias was subtracted, the pixel-to-pixel variations were rectified by division by a mean sky flat field exposure and the data were rebinned into channels of constant wavelength width by fitting third order polynomials to the comparison lamp spectra. The atmospheric extinction was corrected and an absolute flux calibration was applied from the observation of the spectrophotometric standard. Spectra were extracted over the total extent of the nebulae along the slit (large for the NTT observations on account of the poor focus) and the mean sky from along the slit was utilized for sky subtraction.

The Fornax PN was observed with the SAAO 1.9m Cassegrain unit spectrograph and a Reticon photon counting detector (RPCS). 1-d spectra (1024 pixels) of object and offset sky are obtained through two apertures separated by 30″ on the sky of length 6″. Low dispersion spectra with a 210Å/mm grating giving a resolution of 8Å were obtained. A series of six 1200s exposures was obtained alternating the object in each aperture. Exposures of the spectrophotometric standard star LTT 1020 (Hamuy et al. 1994) were obtained in a similar manner. All the data were wavelength calibrated with Cu-Ar lamp exposures. Full details are listed in Table 1. The spectra of the standard and the target were reduced separately for each aperture. After wavelength calibration and extinction correction, sky in the paired aperture was subtracted, the separate spectra averaged and the spectrum flux calibrated by the standard star spectrum in the same aperture. The final spectrum was formed from the averaged spectra from both sets of calibrated aperture spectra.

2.2. Imaging

Accurate J2000 coordinates were determined for both confirmed Sagittarius galaxy PN, and for the possible candidate PRMG-1, and are listed in Table 2.

On the same night as the NTT spectroscopic observations, [O III]5007Å and Hα+[N II] emission line images were obtained of both He 2-436 and Wray 16-423 with EMMI. Table 3 presents the details of the filter observations. The detector was the same as that used for spectroscopy. The NTT observations were obtained in Director's Discretionary Time following telescope and instrument testing. An image analysis had not been performed to set the active optics. The images therefore suffer from poor focus and uncorrected coma. The seeing was in addition not

---

[2] IRAF is distributed by the National Optical Astronomy Observatories, which is operated by the Associated Universities for Research in Astronomy, Inc., under contract to the National Science Foundation.

Table 1: Log of spectrometric observations

Telescope/ Instrument	Object	Lines mm^{-1}	λ range (Å)	Slit width ($''$)	Exp. (s)	Date
NTT/EMMI RILD	He 2-436	360	3800-8400	1.5	1200	1996 May 28
	Wray 16-423	360	3800-8400	1.5	1000	1996 May 28
	Wray 16-423	360	3800-8400	5.0	200	1996 May 28
ESO 1.5m/ B & C	He 2-436	600	3600-7300	2.0	600	1996 June 03
	He 2-436	600	3600-7300	2.0	1800	1996 June 03
	He 2-423	2400	3490-4490	2.0	2400	1996 June 06
	Wray 16-423	600	3600-7300	2.0	180	1996 June 04
	Wray 16-423	600	3600-7300	2.0	1800	1996 June 04
	Wray 16-423	600	3600-7300	6.4	900	1996 June 04
	Wray 16-423	2400	3490-4490	2.0	3600	1996 June 06
SAAO 1.9m/ RPCS	Fornax PN	300	3300-7500	1.8	7200	1990 Sept 22

Table 2: Coordinates of confirmed and possible planetary nebulae in the Sagittarius Dwarf

PN		RA	(J2000)		Dec		Heliocentric velocity (kms^{-1})
	h	m	s	$^\circ$	$'$	$''$	
He 2-436	19	32	06.69	-34	12	57.8	+133
Wray 16-423	19	22	10.52	-31	30	38.8	+133
PRMG-1	21	05	53.57	-37	08	40.7	

good with values in excess of 1″, and the measured seeing (FWHM) of star images was 1.5″. In the limited time available, no flat field frames could be taken nor spectrophotometric calibration stars observed. The images were therefore treated in essentially their raw form.

3. Results

3.1. Spectrometry

All the spectra were analysed by interactively fitting Gaussians to the emission lines. Errors on the line fits were computed taking into account the photon noise on the data, the read-out noise and the underlying continuum and sky, and errors on the lines fluxes were propagated. Within the errors the ESO 1.5m low and intermediate dispersion data were consistent for each PN. However the reddening for He 2-436, determined from the ratios of the observed Balmer lines to the Case B values, for the NTT grism data was larger than the value determined from the ESO 1.5m data. Also no consistent fit to a single value of c was determined from the Hα/Hβ, Hβ/Hγ and Hβ/Hδ ratios for the NTT observations of Wray 16-423.

The NTT data suffered from poor focus which may have affected the spectral transmission, even though the observations were taken at modest zenith distances (29° for the standard, 26° for He 2-436 and 16° for Wray 16-423). The He 2-436 NTT spectrum indicated a consistent, but high, value of the reddening from ratios of Balmer lines and was taken at similar airmass to the spectrophotometric standard, whilst the airmass of the Wray 16-423 observation differed. The different values of reddening remain puzzling but the dereddened spectra from the ESO 1.5m and NTT data for He 2-423 were very similar tending to indicate that there was a systematic (colour) effect for the NTT spectra. Jacoby & Kaler 1993 have discussed in detail the problems encountered in spectrophtometry of faint emission line objects such as PN. In our case the lack of image analysis most probably resulted in the image being centred in the slit only for a narrow range of wavelengths and thus the effects of differential atmospheric refraction were exaggerated. In particular uncorrected coma (which is wavelength dependent) could account for the effects. It was decided to adopt the ESO 1.5m reddening values and use the relative line fluxes in the blue. Where fainter lines were detected in the NTT spectra, or better detections of fainter lines, these values were used, taking the ratio to the nearest strong line; errors were propagated accordingly. In the red ($\lambda \gtrsim$6300Å) the second order contamination affected the ESO 1.5m fluxes, so the NTT fluxes were used in this region scaled to the dereddened Hα flux. Thus the composite spectrum was constructed in dereddened space and then reddened. The Galactic reddening law (Seaton 1979) was used throughout.

Tables 4 and 5 list the resulting observed and dereddened nebular spectra of He 2-436 and Wray 16-423 respectively. The errors are the propagated 1σ errors from the line fits; the sometimes differing error values for lines of similar strength result from the source of the line strengths (ESO 1.5m grating low dispersion (3600-6400Å), ESO 1.5m intermediate dispersion for the 3500-4500Å region and NTT spectrum (4100-8000Å)). Given that the final spectra in Tables 4 and 5 are composites of several individual spectra, there may be small systematic errors which increase slightly the errors above those tabulated. The errors on the reddening have not been propagated to the dereddened relative line intensities in Tables 4 and 5. Table 6 lists the derived parameters from the spectra. Noteworthy is the differing value of c for the two nebulae. He 2-436 has a much higher extinction (by 0.28 in E_{B-V}) than Wray 16-423. The extinction to Wray 16-423 is the same as that for the stellar component of the Sagittarius dwarf (Ibata et al. 1995; Mateo et al. 1995), further corroborating evidence that it is indeed a bona fide member of this galaxy. The higher extinction to He 2-423 is either evi-

Table 3: Log of NTT/EMMI imaging observations

Target Name	Filter Name	Central λ (Å)	Width (Å)	Exp. (s)	Date
He 2-436	[O III]	5013	59	300	1996 May 27
He 2-436	Hα+[N II]	6566	61	300	1996 May 27
Wray 16-423	[O III]	5013	59	200	1996 May 27
Wray 16-423	Hα+[N II]	6566	61	300	1996 May 27

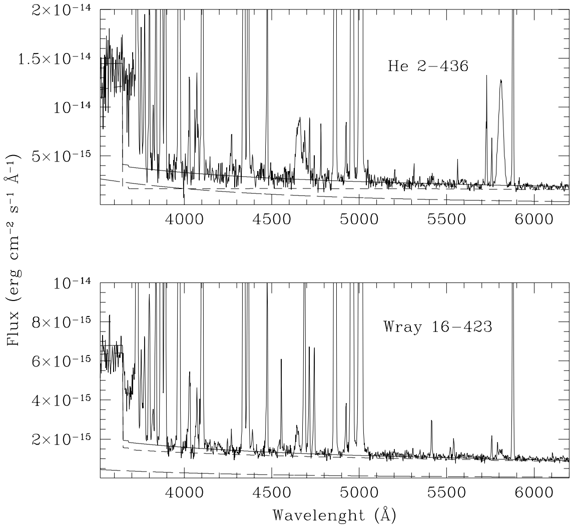

Fig. 1.— (a) The dereddened spectrum (thick bold line), the nebular continuum (short-dashed line), the adopted black body flux (long-dashed line) and the sum of black body and nebular continuum (continuous line) are shown for the fit to the spectrum of He 2-436. (b) The dereddened spectrum, the nebular continuum and the adopted black body flux are similarly shown for Wray 16-423.

dence for patchy extinction along the two line of sight through the Galaxy to this PN or suggests that there is local extinction in He 2-423. Given that He 2-423 is a compact, dense nebula with strong IR emission (it corresponds to the IRAS point source 19288-3419 with well detected 12 and 25μm fluxes), then there is probably a large component of local extinction present.

The absolute observed Hβ flux for Wray 16-423 was determined from the wide slit observation. For He 2-436 no reliable wide slit observation was obtained and the result from Webster 1983 was used. The H I (and for Wray 16-423 the He II) black body Zanstra temperatures were determined from the long exposure (narrow slit) spectra after scaling the total spectrum (line + continuum) by the ratio of the absolute Hβ flux to the observed Hβ flux, reddening correcting the spectra and subtracting the H and He nebula continuum (bound-free, free-free and 2-photon), using the DIPSO analysis package (Howarth et al. 1995). The dereddened stellar B magnitudes were determined from the continuum flux and are listed in Table 6. Figure 1 shows a composite of the dereddened spectra and the nebular and stellar continua; the stellar continuum is shown as a black body of temperature 60000K for He 2-436 and 90000K for Wray 16-423.

Table 4

Observed and reddening corrected spectrum of He 2-436

λ (Å)	IDENTIFICATION	OBSERVED		DEREDDENED	
		FLUX	ERROR	FLUX	ERROR
3704	H I (B16)	2.70	0.90	3.90	1.29
3712	H I (B15)	2.97	0.66	4.28	0.95
3722	H I (B14)	3.08	0.48	4.42	0.69
3726	[O II]	5.36	0.44	7.68	0.63
3728	[O II]	2.18	0.61	3.13	0.87
3734	H I (B13)	2.06	0.46	2.95	0.66
3749	H I (B12)	4.54	0.70	6.47	0.99
3770	H I (B11)	3.72	0.75	5.28	1.07
3798	H I (B10)	3.99	0.57	5.62	0.81
3820	He I	0.86	0.37	1.21	0.51
3836	H I (B9)	5.57	0.34	7.76	0.47
3869	[Ne III]	41.75	0.75	57.70	1.04
3889	H I (B8) + He I	13.37	0.38	18.37	0.52
3967	[Ne III]	13.92	0.49	18.71	0.66
3970	Hϵ (B7)	11.97	0.45	16.08	0.60
4026	He I	2.65	0.35	3.50	0.46
4068	[S II]	2.13	0.44	2.78	0.57
4076	[S II]	0.75	0.34	0.98	0.44
4101	Hδ (B6)	20.26	0.44	26.15	0.56
4267	C II	0.79	0.19	0.97	0.23
4340	Hγ (B5)	39.17	0.59	46.79	0.70
4363	[O III]	12.07	0.24	14.31	0.29
4471	He I	5.34	0.19	6.11	0.21
4712	[Ar IV] + He I	1.49	0.18	1.57	0.19
4740	[Ar IV]	0.71	0.13	0.74	0.14
4861	Hβ (B4)	100.00	0.00	100.00	0.00
4921	He I	1.67	0.13	1.63	0.13
4959	[O III]	281.03	1.32	271.64	1.28
5007	[O III]	831.72	3.45	790.83	3.28
5517	[Cl III]	0.26	0.11	0.21	0.09
5537	[Cl III]	0.17	0.08	0.13	0.07
5755	[N II]	1.44	0.12	1.10	0.09
5876	He I	24.62	0.22	18.21	0.16
6301	[O I]	7.28	0.07	4.90	0.05
6312	[S III]	3.68	0.05	2.47	0.03
6364	[O I]	2.71	0.06	1.80	0.04
6548	[N II]	5.54	0.71	3.54	0.45
6563	Hα (B3)	442.54	1.49	282.16	0.95
6583	[N II]	18.00	0.54	11.43	0.34
6678	He I	7.17	0.08	4.47	0.05

TABLE 4—*Continued*

λ (Å)	IDENTIFICATION	OBSERVED FLUX	OBSERVED ERROR	DEREDDENED FLUX	DEREDDENED ERROR
6717	[S II]	0.79	0.05	0.49	0.03
6731	[S II]	1.79	0.04	1.11	0.03
7065	He I	22.13	0.34	12.84	0.20
7136	[Ar III]	11.31	0.25	6.48	0.14
7235	[Ar IV]	1.60	0.06	0.90	0.03
7254	O I	0.23	0.06	0.13	0.03
7281	He I	1.92	0.06	1.07	0.03
7320	[O II]	11.23	0.08	6.24	0.05
7330	[O II]	12.68	0.08	7.03	0.05
7749	[ArIII]	2.34	0.06	1.22	0.03
7818	He I	0.50	0.05	0.26	0.03

Table 5

Observed and reddening corrected spectrum of Wray 16-423

λ (Å)	IDENTIFICATION	OBSERVED FLUX	OBSERVED ERROR	DEREDDENED FLUX	DEREDDENED ERROR
3686	H I (B19)	0.57	0.27	0.65	0.30
3691	H I (B18)	0.72	0.29	0.82	0.32
3697	H I (B17)	1.02	0.25	1.15	0.28
3704	H I (B16)	1.75	0.30	1.97	0.34
3712	H I (B15)	1.86	0.30	2.09	0.34
3723	H I (B14)	4.20	0.26	4.73	0.29
3726	[O II]	16.55	0.25	18.62	0.29
3728	[O II]	7.86	0.24	8.84	0.27
3734	H I (B13)	2.44	0.28	2.74	0.32
3750	H I (B12)	2.68	0.33	3.02	0.37
3754	O III	0.86	0.37	0.96	0.41
3760	O III	1.00	0.25	1.12	0.28
3770	H I (B11)	3.71	0.25	4.16	0.28
3798	H I (B10)	4.50	0.27	5.03	0.30
3819	He I	1.14	0.23	1.27	0.25
3835	H I (B9)	6.24	0.25	6.96	0.28
3868	[Ne III]	66.73	0.67	74.20	0.74
3889	H I (B8) + He I	16.72	0.25	18.56	0.27
3967	[Ne III]	21.31	0.21	23.48	0.23
3970	Hϵ (B7)	12.14	0.16	13.37	0.18
4026	He I	2.62	0.21	2.88	0.23
4069	[S II]	1.93	0.24	2.10	0.26
4076	[S II]	0.61	0.17	0.66	0.18
4101	Hδ (B6)	23.58	0.25	25.64	0.27
4143	He I	0.68	0.23	0.74	0.25
4267	C II	0.46	0.14	0.49	0.15
4340	Hγ (B5)	44.69	0.21	47.38	0.22
4363	[O III]	12.92	0.20	13.67	0.21
4387	He I	0.70	0.09	0.74	0.10
4471	He I	5.20	0.22	5.43	0.23
4517	C III?	3.39	0.18	3.52	0.19
4541	He II	0.31	0.07	0.32	0.08
4569	[Mg I]	0.30	0.09	0.31	0.10
4685	He II	11.14	0.13	11.36	0.13
4712	[Ar IV] + He I	2.99	0.08	3.04	0.09
4740	[Ar IV]	2.86	0.07	2.90	0.08
4861	Hβ (B4)	100.00	0.00	100.00	0.00
4922	He I	1.34	0.07	1.33	0.07
4959	[O III]	377.21	0.99	373.07	0.98
5007	[O III]	1102.69	2.71	1084.79	2.67

In Table 7 the observed and dereddened spectra of the Fornax PN are presented. The flux measurements are not of high quality; the extinction is zero to within the error and the [O III]4363Å line was not detected, nor were the [S II]6716+6731Å lines. The relative fluxes are, within the errors, generally consistent with those presented by Danziger et al. (1978) with the exception of the [N II] 6583Å line which is 35% stronger (compared to [O II]3727Å) than measured by Danziger et al. (1978) based on deblending of the [N II] line from Hα. Until improved data are available, and in particular a determination of the electron density, the abundances presented by Maran et al. (1984), based on the Danziger et al. (1978) fluxes, will be used, with exception of the N abundance which is increased by 35%.

Figure 2 shows N_e - T_e diagnostic diagrams for He 2-436 and Wray 16-423. For Wray 16-423 there is a fairly well defined intersection region between the [O III]5007/4363Å, [N II]6583/5755Å and [Ar IV]4711/4740Å, [Cl III]5517/5537Å, [S II] and [O II] diagnostic ratios; taking account of the errors in the ratios, values for T_e of 12400K and N_e of 6000cm^{-3} were adopted. For He 2-436, the [O II] and [S II] diagnotics shows densities close to the critical densities for the upper levels of various transitions. The only reliable intersection is for the [O III], [N II] and [O II]7325/3727Å ratio; the adopted values of T_e and N_e are 12600K and 1.1×10^5 respectively. Estimated errors on T_e and N_e for both nebulae are listed in Table 6. Considering the observational errors and their propagation to the derived diagnotic parameters, it was not considered warranted to distinguish two electron temperature regimes as measured from the [O III] and [N II] diagnostic ratios. Ionized masses of both nebulae were calculated from the absolute Hβ fluxes and the adopted electron densities and are listed in Table 6.

Using the adopted diagnostics, the abundances of the elements were derived for the forbidden line species from five level atoms calculations using the NEBULA package (Shaw & Dufour 1995). For He I the recent recombination coefficients of Smits (1996) were used and for He II the values tabulated by Osterbrock (1989). Using standard ionization correction factors (Barker 1983 and Kingsburgh & Barlow 1994), the total abundances of He, O, N, Ne, S, Ar were derived and are listed in Table 8 with the maximum one-sided errors (based on propagated errors in both T_e and N_e and the line ratios). The total C abundance is not listed in Table 8, since only the C II 4267Å recombination line was observed; this line is notoriously unreliable for C/H determination (see Rola & Stasińska 1995). The 4267Å line was detected in both nebulae (signal-to-noise >3) and in multiple spectra. The C^{2+}/O^{2+} ratio ($\approx$ C/O) is 7.8±2.3 for He 2-436 and 3.4±1.2 for Wray 16-423 (errors from the C II/[O III] line ratio), indicating that both PN may be carbon rich. This would not be surprizing given that there are carbon stars observed in the Sagittarius galaxy (Whitelock et al. 1996) and a carbon Mira has been discovered (Whitelock, 1997, private communication). Maran et al. (1984) determined that the PN in Fornax is also carbon rich (C/O=3.7), using a measurement of the forbidden C III] doublet at 1908Å.

3.2. Imaging

For both the [O III] and Hα images, a bright unsaturated star image was selected and used as the PSF for a Richardson-Lucy restoration of the region around the PN images. 100 iterations of the Lucy (1974) iterative deconvolution were performed. The image of He 2-436 appeared stellar (i.e. unresolved) in both filter images, implying a diameter $<1''$. For Wray 16-423, the source appeared to be elliptical with a major axis of $1.2''$ and axial ratio 0.7 in position angle $\sim 50°$. Adopting another star in the field for the PSF did not alter these results significantly. Higher resolution (e.g. HST) images are required to resolve both nebulae and give more information on their morphology.

Table 5—*Continued*

λ (Å)	IDENTIFICATION	OBSERVED FLUX	OBSERVED ERROR	DEREDDENED FLUX	DEREDDENED ERROR
5048	He I	0.22	0.06	0.22	0.06
5412	He II	1.03	0.06	0.97	0.05
5518	[Cl III]	0.27	0.05	0.25	0.04
5538	[Cl III]	0.37	0.04	0.34	0.04
5755	[N II]	0.58	0.06	0.53	0.06
5795	He II	0.40	0.03	0.37	0.03
5814	He II	0.20	0.04	0.19	0.04
5876	He I	18.07	0.10	16.37	0.09
6103	[K IV]	0.15	0.04	0.14	0.04
6302	[O I]	2.41	0.07	2.12	0.06
6313	[S III]	2.05	0.07	1.80	0.06
6366	[O I]	0.94	0.06	0.83	0.05
6550	[N II]	6.30	0.06	5.44	0.05
6563	Hα (B3)	329.14	0.83	284.02	0.72
6586	[N II]	20.58	0.09	17.73	0.08
6680	He I	4.66	0.20	3.99	0.17
6719	[S II]	1.79	0.10	1.53	0.09
6733	[S II]	3.36	0.09	2.86	0.07
7065	He I	8.74	0.10	7.31	0.08
7138	[Ar III]	11.71	0.12	9.76	0.10
7236	[Ar IV]	0.44	0.05	0.37	0.04
7263	[Ar IV]	0.12	0.04	0.10	0.03
7281	He I	0.99	0.08	0.82	0.06
7321	[O II]	2.50	0.06	2.06	0.05
7331	[O II]	3.18	0.06	2.62	0.05
7750	[Ar III]	2.29	0.05	1.85	0.04

Table 6: Physical parameters of Sagittarius PN

Parameter	He 2-436		Wray 16-423	
	Value	Error	Value	Error
c	0.61	0.05	0.20	0.04
E_{B-V} (mag.)	0.42	0.03	0.14	0.03
$\mathrm{Log}_{10}F(H\beta)^{a}$	-12.17[b]	0.03	-12.09	0.03
$\mathrm{Log}_{10}F(H\beta)^{c}$	-11.56	0.06	-11.89	0.04
T_e (K)	12600	400	12400	400
N_e (cm^{-3})	1.1×10^5	0.3×10^5	6000	1500
Ionized mass ($M_\odot$)	0.016		0.14	
$T_{Zanstra}$ (H I)	61000		85000	
$T_{Zanstra}$ (He II)			96000	
B (mag.)[d]	16.7		18.7	
$L_\odot$	5300		2300	

---

[a] Observed flux

[b] Absolute observed Hβ flux and error from Webster (1983)

[c] Dereddened flux

[d] Corrected for extinction

Table 7: Observed and redenning corrected spectrum of Fornax PN

λ (Å)	IDENTIFICATION	OBSERVED		DEREDDENED	
		FLUX	ERROR	FLUX	ERROR
3727	[O II]	35	6	34	6
3869	[Ne III]	45	5	43	4
3889	H I (B8) + He I	22	4	21	4
3970	[Ne III] + Hϵ (B7)	25	4	24	3
4101	Hδ (B6)	28	3	27	3
4340	Hγ (B5)	38	3	37	3
4861	Hβ (B4)	100	0	100	0
4959	[O III]	179	7	180	7
5007	[O III]	548	19	551	19
5876	He I	12	2	13	2
6563	Hα (B3)	271	21	285	12
6583	[N II]	12	3	13	3

NOTE.—Reddening c=−0.07±0.13 (E_{B-V}=-0.04)

4. Discussion

4.1. Abundances of PN in dwarf elliptical galaxies

Table 8 contrasts the abundances of the light elements measured in the two PN in the Sagittarius dwarf elliptical with that in the Fornax dwarf galaxy (from Maran et al. 1984). The similarity in abundances of O, Ne, S and Ar of the two PN in the Sagittarius dwarf can be regarded as independent evidence, in addition to the dynamical data, that both Wray 16-423 and He 2-436 do belong to the Sagittarius Dwarf galaxy. The abundance values listed for Fornax in Table 8 must be considered more uncertain in view of the lack of a direct measurement of the electron density in this nebula. The striking aspect is that the O, Ne and Ar abundances are identical within the errors between the Fornax PN and the Sagittarius PN. This level of similarity strongly suggests that all three PN were formed within a common evolutionary scenario and, since they arise in similar mass stellar systems, at similar evolutionary times. The largest discrepancy between these three PN is for N, where the N abundance of He 2-436 is very low. However the ionization correction factor is large for this element and the diagnostic diagram shows a range of physical conditions; a lower electron temperature and or a higher electron density in the low ionization zone would increase the N abundance. The abundances are much lower (by 0.5 dex on average) than Galactic PN as indicated by the comparison in Table 8 with the mean abundance for 42 non-Type I (i.e. from low mass progenitors) Galactic PN from Kingsburgh & Barlow (1994). Solar abundances are included for comparison in Table 8 (column 9).

Confirmation that He 2-436 and Wray 16-423 do belong to the Sagittarius dwarf can be sought by comparing the nebular abundances with those of the stellar population. The PN abundances give a mean depletion of -0.7 with respect to Solar ([X/H]). However in the case of the stars there appears to be a wide range of metallicities so direct comparison of PN and stellar metallicities is equivocal. Sarajedini & Layden (1995) found two populations at [Fe/H] = -0.52 and -1.2, as well as a more metal-poor population associated with M 54; Mateo et al. (1995) found a mean metallicity of [Fe/H] = -1.1 and Whitelock et al. (1996) a mean value of [Fe/H] = -0.8. Marconi et al. (1997) observed a spread in [Fe/H] between -0.7 and -1.58, with a dominant population similar to the cluster Terzan 7 and Ibata et al. (1997) measured a metallicity range between [Fe/H] = -0.8 and -1.0. It can be concluded that the Sagittarius PN progenitors are representative of the higher metallicity tail of the Sagittarius population. Choosing as compromise a mean [Fe/H] of -0.8, leads to a relative oxygen abundance of [O/Fe] = +0.2 for Sagittarius.

It is natural to compare the abundances of the Sagittarius and Fornax PN with those of the 'halo' PN. The halo PN are not a well defined group, being selected on the basis of either position away from the Galactic plane, high velocities and or low abundances. Their abundances vary over a rather wide range so it is not appropriate to form a mean abundance set (see Howard et al (1997) for an abundance analysis of 9 halo PN). Clegg et al. (1987) compared the abundances of three halo objects H 4-1 (PN G 049.3 +88.1), BoBn-1 (PN G 108.4 -76.1) and DdDm-1 (PN G 061.9 +41.3). It is clear that the abundances of the Fornax and Sagittarius PN closely resemble those of DdDm-1 to a remarkable degree, and this PN is included in Table 8 (data from Clegg et al. 1987). The possible candidate PN in Sagittarius, PRMG-1 (PN G 006.0 −41.9), is included in Table 8 although the N and S abundances are limits only; the abundances are also similar to the Sagittarius and Fornax PN. Barker & Cudworth (1984) have suggested that S and Ar, which should not be affected by the AGB nuclear processing, should be representative of the heavy element abundance of the parent material. The similarity in abundances of the Sagittarius and Fornax PN and DdDm-1 in these elements confirm their origin in a population which did not undergo large element enrichment from supernova products. In contrast the abundances of all elements are much higher, by ∼0.8dex, than for K 648, the PN in the metal poor Galactic globular cluster M 15 (Adams et al. 1984), which is also listed in Table 8.

In PN with low mass progenitors (non Type I), the abundance of O is only marginally affected by AGB evolution (≤0.2dex, e.g. Kingsburgh & Barlow 1994). However, the sum of C, N and O should change little through the AGB evolution. The increase in carbon is due to triple-α reactions, the products of which are brought to the surface by the 3rd dredge-up. Assuming that the derived C/O abundances from the C II 4267Å line are fairly reliable for the Sagittarius PN, both show excess carbon indicating that He shell flashes have occured. The C abundance of the Fornax PN is more reliable and shows a similar level at C/H of $1{\times}10^{-3}$. In contrast DdDm-1 shows low carbon abundance (12+Log(C/H)<7.1, Clegg et al. 1987) and it has been suggested that most of the C was converted into N and that mass loss of the low mass core terminated after only early AGB evolution (Clegg et al. 1987). The high carbon abundance in the dwarf galaxy PN suggest that these stars have progressed through a number of thermal pulses and suffered He shell burning. The lower N abundance for He 2-436 could be due to relatively little carbon being burnt to N (the 12+Log(C/H) abundance of He 2-436 is 9.2, whilst it is 8.8 for Wray 16-423, taking the C/O ratios at face value).

The fundamental question to be answered is: what do the abundances of the PN in the Sagittarius and Fornax dwarf galaxies tell us about the progenitor stars from which they were formed, and further, what do they reveal of the evolutionary history of these galaxies. The similarity of S and Ar abundances with the SMC PN abundances (Monk et al. 1988) is striking and, together with the proposal that the Sagittarius galaxy is quite massive (Ibata et al. 1997), suggests that the difference between the SMC and Sagittarius can partly be understood in terms of gas being stripped from Sagittarius and with little interaction occurring with gas clouds, in contrast to the SMC. The fact that the PN abundances are almost as low as in the more metal rich blue compact galaxies (such as II Zw 40, Walsh & Roy 1993 and NGC 2363, Peimbert et al. 1996) suggests that these satellite galaxies could be related objects with a different history of gas infall. If the elevated oxygen abundance of the Sagittarius and Fornax PN relative to K 648 in M 15 is a guide, then the Sagittarius and Fornax systems are not simply agglomerations of Galactic globular clusters. The similarity between the abundances of the two Sagittarius PN and those of PRMG-1 (Pĕna et al. 1989), suggests that the latter PN could also belong to the Sagittarius dwarf. If PRMG-1 does belong to the Sagittarius galaxy and is still bound, then the extent of the galaxy is much larger than found by Ibata et al. (1997). DdDm-1 also has similar abundances, but due to its location it would be premature to suggest that it was once a member of the Sagittarius dwarf. The similarity of abundances between the Sagittarius and Fornax PN and some halo PN suggests that some halo stars could have been been captured from satellite dwarf galaxies such as Sagittarius and Fornax.

The [O/Fe] value for the Sagittarius dwarf has implications for the metal enrichment history of this galaxy. An [O/Fe] value significantly higher than Solar would rule out Sagittarius as a dwarf irregular galaxy, but taking account of the spread in [Fe/H] deduced from the various published determinations, this argument is weakened. The presence of a wide metallicity range indicates star formation at different times. Several pieces of evidence point towards the notion that Sagittarius was more massive in the past: it falls below the luminosity-metallicity relation of Lee (1995); it is being disrupted by the Milky Way (Piatek &

Pryor 1995; Velazquez & White 1995; Johnston et al. 1995); it may have had an escape velocity high enough to retain the gas and form successive generations of stars (Ibata et al. 1997). The fact that [O/Fe] is $\sim +0.2$ would argue against significant enrichment from SN type I. In an isolated dwarf galaxy, this value would favour a SN driven wind followed by recapture of the enriched gas with subsequent star formation. Thus, the available element ratios are not inconsistent with two bursts of star formation, although the star formation history of Sagittarius must be unusual. In particular, this history may not be directly compared to that of other more distant dwarfs that have not suffered severe interactions with the Milky Way. The interation with the Galaxy may have caused the gas to escape after a few orbits, and it may have caused prior bursts of star formation.

4.2. The central stars of the Sagittarius PN

Both He 2-436 and Wray 16-423 show Wolf-Rayet (WR) features in their spectra. Figure 3 shows part of the low dispersion ESO 1.5m spectra at the flux levels of the broad stellar lines. Table 9 lists the observed equivalent widths, line widths (FWHM corrected for instrumental width) and fluxes: He 2-436 shows strong C IV 4658 and 5810Å and weaker N III 4640Å and He II 4686Å, but no C III lines (4650 and 5695Å) were detected; Wray 16-423 shows weak N III 4640Å, C III 4650Å and C IV 5810Å, barely detected C III 5695Å, but no detectable broad He II 4686Å emission. On the basis of the relative line strengths He 2-436 is classified as type [WC3-4] since it has strong C IV, lack of C III and no O V or O VI; Wray 16-423 is classified as type [WC8] on the basis of the similar strengths of the C III and C IV lines and absence of O V (c.f. the WR classification of PN by Tylenda et al. 1993). However this classification goes in the opposite sense to that expected from the Zanstra temperatures of both stars (Table 6): He 2-436 has an earlier [WC] class but a lower temperature, whilst Wray 16-423 has a later spectral class but considerably higher stellar temperature. The weak and narrower lines of Wray 16-423 would lead to its classification as a "weak emission line central star" by Tylenda et al. (1993), so it may be somewhat misleading to directly compare both stars. However the discrepancy is puzzling when considered simply in terms of ionization - the hotter star appears to produce a lower ionization wind than the cooler star. This effect remains unexplained but could possibly be due to different line blanketing in the two stars.

The Wolf-Rayet characteristics of the two central stars give important constraints on their evolutionary status. Central stars of planetary nebulae (CSPN) mostly evolve either on hydrogen-burning (Schönberner 1983) tracks or on helium-burning tracks, before entering the white-dwarf cooling phase. The track for a given object depends on the phase of the thermal-pulse cycle at which the central star leaves the AGB. Since the hydrogen-burning phase lasts several times longer than the helium-burning one, most CSPN are assumed to belong to the former category. In contrast, since the Wolf-Rayet CSPN are known to be hydrogen poor, there is little doubt that they are presently in a helium-burning phase (e.g. Pottasch 1996). The wind emission lines, which are the defining characteristics of WR stars, are expected to disappear on the white-dwarf cooling track: the luminosity quickly drops by a factor of 100, far below the Eddington luminosity. Consequently, [WC] stars will still be on the nuclear-burning part of their evolution.

Compared to the Schönberner tracks (Schönberner 1983), which assume quiescent hydrogen burning, helium burners are expected to deviate in their evolutionary time scales and luminosity evolution (Iben 1984). Detailed calculations of evolutionary tracks including helium-burning phases have been made by Vassiliadis & Wood (1993) but these are not yet comprehensive. Whereas quiescent hydrogen burners are described by the

Table 8

Comparison of abundances for dwarf elliptical galaxy and Galactic PN

Element[t]	He 2-436	Wray 16-423	Fornax[u] PN	DdDm-1[v]	PRMG-1[w]	K 648[x]	Galactic PN[y]	Solar[z]
He	11.02±0.02	11.03±0.02	11.08	11.0	10.96	11.02	11.05	10.99
N	6.97±0.16	7.62±0.10	7.5	7.4	<8.3	6.5	8.14	8.00
O	8.29±0.08	8.31±0.07	8.4	8.1	8.06	7.67	8.69	8.93
Ne	7.57±0.08	7.50±0.08	7.6	7.3	7.23	6.7	8.10	8.09
S	6.30±0.08	6.48±0.08		6.5	<7.00	5.2	6.91	7.24
Ar	5.76±0.12	5.88±0.08	5.9	5.8	5.50	4.3	6.38	6.57

[t] $12 + \mathrm{Log}_{10}(\mathrm{Abundance/H})$

[u] Fornax PN O, Ne and Ar abundances from Maran et al. (1984)

[v] DdDm-1 abundances from Clegg et al. (1987)

[w] PRMG-1 abundances from Howard et al. (1997)

[x] K 648 abundances from Adams et al. (1984), except for S and Ar from Barker & Cudworth (1984)

[y] Mean composition for 42 non-Type I Galactic PN from Kingsburgh & Barlow (1994)

[z] Solar abundances from Anders & Grevesse (1989)

Table 9: Parameters of stellar emission lines in He 2-436 and Wray 16-423

Target	λ(Å)	IDENT.	EW(Å)	FWHM(Å)	Flux[x]
He 2-436	4640	N III	-15.3	12.3	3.7
	4658	C IV	-55.4	23.0	13.4
	4686	He II	-23.7	13.4	5.7
	5810	C IV	-164.6	31.1	32.9
Wray 16-423	4640	N III	-12.7	13.1	1.0
	4650	C III	-5.4	9.9	0.45
	5810	C IV	-5.8	14.7	0.42

---

[x] Observed flux in ergs $\mathrm{cm}^{-2}\mathrm{s}^{-1}\ \times 10^{-14}$.

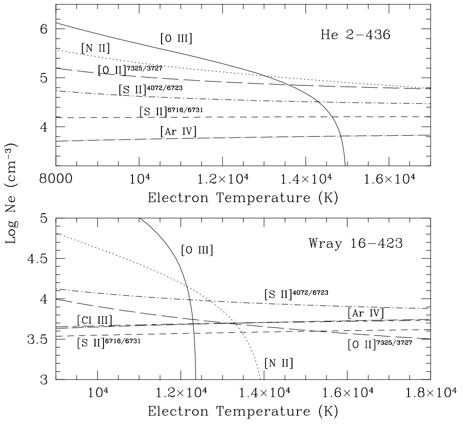

Fig. 2.— N_e - T_e diagnostic diagrams for He 2-436 and Wray 16-423 are shown. The line ratios from which the diagnostic curves are derived are indicated. For ratios not indicated the following holds: [O III] = 5007/4363Å; [N II] = 6583/5755Å; [Ar IV] = 4711/4740Å; [Cl III]5517/5537Å.

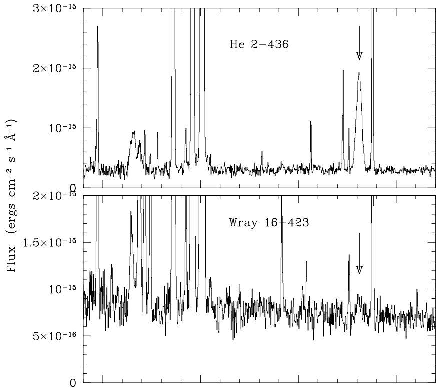

Fig. 3.— Detail of the continuum spectra of He 2-436 and Wray 16-423 is shown. The broad stellar lines of C IV 5810Å are arrowed and the complex of broad lines from C III, C IV, N III and He II is visible around 4600Å, although weaker in Wray 16-423 where they are confused by the strong nebular lines.

core mass as the single major free parameter, helium burners need in addition the phase of the thermal-pulse cycle which measures where on the evolution the thermal pulse occured. In addition, the models assume the presence of an inert hydrogen layer above the helium layers. In the [WC] stars this layer is absent. As a consequence they are not expected to be well described by present models (Schönberner 1996, Schönberner 1997) and extreme care has to be taken in using helium tracks to describe Wolf-Rayet central stars. One of the most favored scenarios for forming hydrogen-deficient central stars is the so-called "very late" thermal pulse, whereby the helium-flash starts after the cessation of hydrogen-burning (i.e. when the star is on the white dwarf cooling track). The convective mixing that later occurs transports any remaining hydrogen downwards into hotter layers where it is burned. The C and O surface abundances predicted in this scenario do not however agree with the observed ones (Schönberner 1996). Evidence for the presence of helium-burning central stars among planetary nebulae in the LMC has been presented by Dopita et al. (1997).

Helium-burning central stars are expected to evolve on tracks of decreasing luminosity towards higher stellar temperatures. The final thermal pulse can occur at the tip of the AGB or during the post-AGB evolution. Immediately following the thermal pulse, the evolution is very fast (Vassiliadis & Wood 1993), and stars in an early phase after the thermal pulse may show up as bright infrared sources (Zijlstra et al. 1994). Subsequently, during quiescent helium burning, they evolve about three times slower than hydrogen-burning stars of the same core mass. However the Wolf-Rayet wind has little effect on the chemical composition of the nebula: during the time of heaviest mass loss following the thermal pulse, the mixing which causes the disappearance of the hydrogen envelope has not yet begun. Galactic planetary nebulae surrounding [WC] stars do not show differences in their abundance patterns (Pottasch 1996, Gorny & Stasinska 1995).

The stellar luminosities of both PN are listed in Table 6 based on the magnitudes and black body temperatures of the central stars. An estimate of the error on the derived luminosities is 20%, resulting from the errors on the extinction, the magnitude and the black body temperature. For He 2-436, a lower limit to the luminosity can be derived by integration of the 12 and 25μm fluxes and the upper limits to the 60 and 100μm IRAS fluxes; a value of 4600$L_\odot$ is derived, consistent with the value in Table 6. Helium-burning central stars can explain why the two Sagittarius PN have luminosities which differ by a factor of 2 (Table 6). The models for helium-burning central stars (assuming an inert upper layer of hydrogen) show that their luminosity along an evolutionary track decreases by upto a factor of 0.6 dex, whereas hydrogen-burning central star models keep a constant luminosity before entering their cooling track. The two PN are expected to have similar core masses: for progenitor masses of 1 $M_\odot$ and lower, the final mass is strongly peaked around a value of approximately 0.55 $M_\odot$ with very small dispersion (Weideman 1987). Only for stars of twice solar and higher masses are significantly higher final masses expected. For hydrogen-burning tracks this would lead to similar luminosities as well, excluding the white-dwarf cooling track. The different luminosities indicate that at least one (the one with the lower luminosity) is not evolving on a track of quiescent hydrogen burning. The position on the HR diagram indicates that neither star has entered the white-dwarf cooling track.

He 2-436 has a higher luminosity than Wray 16-423 and the central star is cooler. The nebula is still young, as indicated by its high density, low ionized mass (Table 6), compact angular size (unresolved in our images) and strong infrared emission; it has shown fast evolution from the AGB. One can hence infer that the star is in an early post-helium-flash evolution. Its luminosity should still be close to the corresponding hydrogen-burning phase. Assuming therefore the hydrogen core mass–luminosity relation of Vassiliadis & Wood (1993), a core mass of 0.59 $M_\odot$ is indicated. Wray 16-423 is more evolved, based on the lower luminosity, lower density and larger angular size (the nebula is resolved with a diameter of 1.2″), as well as lack of infrared emission. Assuming an expansion velocity of 15 km s^{-1} (Zijlstra & Walsh 1996) and using the distance of 25 kpc to the Sagittarius dwarf galaxy, a dynamical age of 4000 years can be deduced for Wray 16-423. Competing factors contribute to the large uncertainty that should be assigned to this figure. As the PN shell enters its energy-driven phase (Kahn & Breitschwerdt 1990), the pressure due to the hot shocked gas filling the inner cavity can accelerate the shell. On the other hand, the outer parts of the shell trace the material expelled during the early superwind phase when the wind velocity might have been lower: the details of the velocity law along the superwind phase are not known.

The models of Vassiliadis & Wood (1993) or Blöcker (1995a, 1995b) give estimates for the transition time from the tip of the AGB to the post-AGB phase and then for the evolutionary time scale on their tracks. The uncertainty on the former quantity is quite large due to different definitions of the end of the AGB between these authors and even changes quite substantially between the models. A dynamical age of 4000 years is still consistent with the time scale needed by a 1 $M_\odot$ star to evolve from the top of the AGB to the actual position of the Sagittarius PN central stars on a log L–log T_{eff} diagram. Provided that the comparison to helium-burning tracks is relevant one can conclude that although no single track in Vassiliadis & Wood (1993) can be uniquely identified with both PN, observationally the results are consistent with Wray 16-423 and He 2-436 evolving on the same track.

Wolf-Rayet central stars make up about 10-15% of the Galactic PN population. They are found both in the disk and bulge, but none are known in the Galactic halo. This indicates a difference between halo/globular cluster PN population (no [WC] stars among ten known PN) and Sagittarius (two out of two). However the presence of weak emisssion line stars, such as Wray 16-423, requires deep spectra and broad stellar features may have been missed. This difference between halo PN and those in Sagittarius could be explained if the halo PN have somewhat lower luminosities, and are therefore unable to sustain a wind. The fact that, from stellar population studies (Mateo et al. 1996), the bulk of the stellar population in Sagittarius appears younger than the Galactic halo is consistent with this. Metallicity might also be a factor, however at this stage of evolution the stellar abundances are dominated by self-produced metals. A possible explanation of the lack of [WC] stars in the halo is that the [WC] phase at lower core mass could be more confined to the high-luminosity peak following the thermal pulse where evolution is very fast.

4.3. Sagittarius as a dwarf elliptical galaxy

The Sagittarius dwarf is now heavily distorted by the tidal field of the Milky Way (e.g. Ibata et al. 1997, Piatek & Pryor 1995), making it difficult to decide its original type. Even though it appears to have a substantial fraction of intermediate-age stars (e.g. Sarajedini & Layden 1995, Mateo et al. 1996), the galaxy presently contains no neutral hydrogen (Koribalski et al. 1994), an argument favouring a dwarf elliptical over a dwarf irregular galaxy. The gas could have been stripped by its many passages through the plane of the Milky Way (Ibata et al. 1997). Figure 4 shows the [O/Fe] abundance ratio plotted against the logarithmic oxygen abundance for the Sagittarius dwarf, together with data for the Milky Way and its satellite galaxies and for the dwarf satellites NGC 185 and NGC 205 of M 31. In this figure the O abundances are derived from the PN and the Fe from the stellar population. The data for NGC 185 and NGC 205 are taken from Richer et al. (1997). For NGC 205 the oxygen abundance is based on lower limits derived from [O III] and Hβ line fluxes for 9 PN (Richer & McCall 1995), whilst for NGC 185 it is based on spectroscopy of two PN. The oxygen data for the Milky Way disk and bulge are from Ratag et al. (1992).

For the Fornax dwarf, Richer & McCall (1995) estimate an oxygen abundance 0.4 dex lower than that measured for the PN (Maran et al. 1984; Danziger et al. 1978) based on the fact that the oxygen abundance is slightly higher for the brightest PN in samples for the LMC, SMC and the Galaxy. However it can be argued that if this is the only PN in this galaxy, which is consistent with the mass of the galaxy (Zijlstra & Walsh 1996), then such a correction is not applicable. A further argument against applying such a correction is that for the two Sagittarius PN, one (He 2-436) is about twice the luminosity of the other whilst their oxygen abundances are very similar. Inferring the oxygen abundance of a stellar population based on a few PN is clearly a complex task and not one that can immediately be referred to more massive galaxies where samples are large and the star formation history may be quite different. The oxygen abundances for NGC 185 and NGC 205 used in Figure 4 have been determined by applying a correction to the lower limits based on the behaviour of Milky Way and Magellanic Clouds PN samples. From Figure 4 it is clear that the [O/Fe] abundance of the Sagittarius galaxy is higher than that in the Magellanic Clouds by a factor of ~ 2, which also argues against Sagittarius having been an SMC-like galaxy.

The Sagittarius PN have somewhat higher abundances than those in the Milky Way halo (see Table 8), typical of younger PN than the halo ones and much higher than K 648. Mateo et al. (1995) argue that the specific frequency of RR Lyrae variables in Sagittarius is low compared with other dwarf elliptical galaxies, which is consistent with a higher metallicity and relative youth of Sagittarius with respect to the halo. This indicates that the halo could not have been made *entirely* of dwarf galaxies such as Sagittarius.

The total absolute magnitude of Sagittarius is unknown. Based on the number of RR Lyrae stars, Mateo et al. (1995) estimated a total magnitude $M_V = -13$, and -11, if Sagittarius had a total of 1930 and 310 RR Lyrae (type ab) stars respectively. Alard (1996) and Alcock et al. (1997) have discovered more than 350 RR Lyrae type ab stars in the northern extension of Sagittarius alone. Their surveys cover at most 1/5 of the total extension of Sgr, judging from the isophotes, so it is concluded that Sagittarius contains $N > 1800$ RR Lyrae type ab stars. Following the arguments of Mateo et al. (1995), a value of $M_V = -13$ is adopted for Sagittarius, which is consistent with a minimum total mass of $10^9 \mathrm{M}_\odot$ (Ibata et al. 1997). Sagittarius also has at least 4 globular clusters (Ibata et al. 1995) but there are a number of globular clusters in the Galactic bulge region (≈30) without velocity or distance information that could also be members. The data accumulated so far (see in particular Ibata et al. 1997) indicates that Sagittarius is at least as massive as Fornax, and it is likely that this galaxy is the most massive of all the dwarf satellite galaxies of the Milky Way.

It is apparent that the oxygen abundance in dwarf elliptical galaxies is higher than for dwarf irregulars at the same absolute magnitude (Richer & McCall 1995), by about a factor of ∼2. Figure 5 shows the dependence of the galaxy luminosity on the oxygen abundance for all the Local Group dwarfs (irregulars and ellipticals) with measured PN or H II region O abundances. This figure shows that, even though the total absolute magnitude of Sagittarius is still uncertain, this galaxy shares the location with the typical dwarf ellipticals NGC 185, NGC 205, and Fornax. It is concluded that the present study of the Sagittarius PN, added to the previous evidence, supports

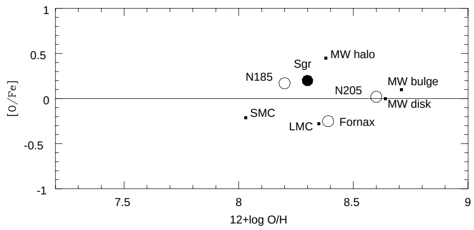

Fig. 4.— Plot of the [O/Fe] abundance ratio versus the logarithmic oxygen abundance (12.0 + $\mathrm{Log}_{10}(\mathrm{O/H})$) for dwarf elliptical galaxies around the Milky Way and M 31. The source of the data for the Milky Way and the M31 satellite galaxies (NGC 185 and 205) is Richer & McCall 1995.

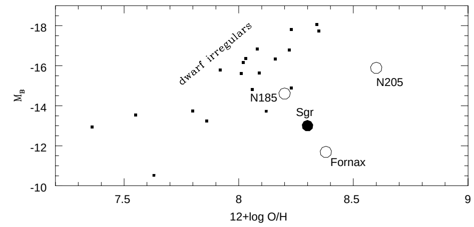

Fig. 5.— Plot of the absolute blue magnitude of the satellite dwarf galaxies of the Milky Way and M 31 against the oxygen abundance (12.0 + $\mathrm{Log}_{10}(\mathrm{O/H})$). The total magnitudes are taken from Richer & McCall 1995 as are the oxygen abundances for the dwarfs except for Sagittarius (this work) and Fornax (oxygen abundance from Maran et al. 1984).

the notion that Sagittarius was not a dwarf irregular, but most probably a dwarf elliptical galaxy.

5. Conclusions

Optical spectra of the two planetary nebulae in the Sagittarius dwarf galaxy have been analysed and the abundances and physical conditions studied. Both PN display similar abundances, differing considerably only for nitrogen. The abundance pattern is also very similar to that for the PN in the Fornax dwarf galaxy. The abundance of oxygen (for example) in these three PN is lower than that of Galactic PN, but not as low as for genuine halo PN, such as the PN in the globular cluster M 15. Broad stellar (WR) lines are seen in both nebulae in Sagitarius with He 2-436 displaying the stronger lines. The luminosity of He 2-436 is about twice that of Wray 16-423 and the latter has a resolved ionized shell. In order to reconcile the different luminosities and evolutionary characterisitics of He 2-423 and Wray 16-423, it is suggested that both are on helium burning evolutionary tracks. The oxygen abundances of the M31 and Milky Way satellite galaxies, as revealed by their planetary nebulae, are compared and the evidence suggests that both Sagittarius and Fornax were not dwarf irregulars but more probably dwarf elliptical galaxies before their interaction with the Milky Way.

The ESO staff at La Silla and the NTT remote observing team in Garching provided excellent support for the observations. We are very grateful to the South African Astronomical Observatory for prompt retrieval of the spectroscopic data for the Fornax PN from their digital archive. We would like to thank the referee, G. H. Jacoby, for many suggestions which substantially improved the paper. The work of D. Minniti was supported in part by Lawrence Livermore National Laboratory, under DOE contract W-7405-Eng-48.

REFERENCES

Acker, A., Ochsenbein, F., Stenholm, B., Tylenda, R., Marcout, J., Schohn, C., 1992, *Strasbourg – ESO Catalogue of Galactic Planetary Nebulae*, ESO

Adams, S., Seaton, M. J., Howarth, I. D., Aurière, M., Walsh, J. R., 1984, MNRAS, 207, 471

Alard, C. 1996, ApJ, 458, L17

Alcock, C., Allsman, R. A., Alves, D. R., Axelrod, T. S., Becker, A. C., Bennett, D. P., Cook, K. H., Freeman, K. C., Griest, K., Guern, J. A., Lehner, M. J., Marshall, S. L., Minniti, D., Peterson, B. A., Pratt, M. R., Quinn, P. J., Rodgers, A. W., Stubbs, C. W., Sutherland, W., Welch, D. L., 1997, ApJ, 474, 217

Anders, E., Grevesse, N., 1989, Geochim. Cosmichim. Acta, 53, 1197

Barker, T., 1983, ApJ, 267, 630

Barker, T., Cudworth, K. M., 1984, ApJ, 278, 610

Blöcker,T., 1995a, A&A, 297, 726

Blöcker,T., 1995b, A&A, 299, 755

Clegg, R. E. S., Peimbert, M., Torres-Peimbert, S., 1987, MNRAS, 224, 761

da Costa, G. S., Armandroff, T. E., 1995, AJ, 109, 2533

Danziger, I. J., Dopita, M. A., Hawarden, T. G., Webster, B. L., 1978, ApJ, 220, 458

Dopita M.A., Vassiliadis E., Wood P.R., Meatheringham S.J., Harrington J.P., Bohlin R.C., Ford H.C., Stecher T.P., Maran S.P., 1997, ApJ, submitted

Gorny S.K., Stasinska G., 1995, A&A, 303, 893

Hamuy, M., Walker, A. R., Suntzeff, N. B., Gigoux, P., Heathcote, S. R., Phillips, M. M., 1994, PASP, 106, 566

Henize, K. G., 1967, ApJS, 14, 125

Howard, J. W., Henry, R. B. C., McCartney, S., 1997, MNRAS, 284, 465

Howarth, I. D., Murray, J., Mills, D., Berry, D. S., 1995, *DIPSO(V3.2) - A friendly spectrum analysis package*, Starlink User Note 50.17

Iben, I., 1984, ApJ, 277, 333

Ibata, R. A., Gilmore, G., Irwin, M. J., 1994, Nature, 370, 194

Ibata, R. A., Gilmore, G., Irwin, M. J., 1995, MNRAS, 277, 781

Ibata, R. A., Wyse, R. F. G., Gilmore, G., Irwin, M. J., Suntzeff, N. B., 1997, AJ, 113, 634

Jacoby, G. H., Kaler, J. B., 1993, ApJ, 417, 209, 1993

Johnston, K. V., Spergel, D. N., Hernquist, L., 1995, ApJ, 451, 598

Kahn, F. D., Breitschwerdt, D., 1990, MNRAS, 242, 505

Kingsburgh, R. L., Barlow, M. J., 1994, MNRAS, 271, 257

Koribalski, B., Johnston, S., Otrupcek, R. 1994, MNRAS, 270, L43

Lee, M. G., 1995, AJ, 110, 1129

Lucy, L. B., 1974, AJ, 79, 745

Marconi, G., Buonanno, R., Castellani, M., Iannicola, G., Molaro, P., Pasquini, L., Pulone, L., 1997, A&A, in press

Mateo, M., Udalski, A., Szymański, M., Kalužny, J., Kubiak, M., Krzemínski, W., 1995, AJ, 109, 588

Mateo, M., Mirabel, N., Udalski, A., Szymaǹski, M., Kalužny, J., Kubiak, M., Krzemínski, W., Stanek, K. Z., 1996, ApJ, 458, L13

Maran, S. P., Gull, T. R., Stecher, T. P., Aller, L. H., Keyes, C. D., 1984, ApJ, 280, 615

Minniti, D., Meylan, G., Kissler-Patig, M. 1996, A&A, 312, 49

Monk, D. J., Barlow, M. J., Clegg, R. E. S., 1988, MNRAS, 234, 583

Osterbrock, D. E., 1989, Astrophysics of Gaseous Nebulae and Active Galactic Nuclei. Mill Valley, University Science Books

Peña, M., Ruíz, M. T., Maza, J., González, L. E., 1989, Revista Mexicana Astron. Astrophys, 17, 25

Peimbert, M., Peña, M., Torres-Peimbert, S., 1986, A&A, 158, 266

Piatek, S., Pryor, C. 1995, AJ, 109, 1071

Pottasch S.R., 1996, Ap&SS, 238, 17

Ratag, et al, 1992, A&A, 255, 255

Richer, M. G., McCall, M. L., 1995, ApJ, 445, 642

Richer, M. G., McCall, M. L., & Arimoto, N. 1997, A&A, in press

Rola, C., Stasińska, G., 1995, A&A, 282, 199

Sarajedini, A., Layden, A. 1995, AJ, 109, 1089

Schönberner, D., 1983, ApJ, 272, 708

Schönberner, D. (1996) Hydrogen Deficient Stars, eds. U. Heber, S. Jeffrey, ASP Conf. Ser., 96 p. 433

Schönberner D., 1997, in IAU Symp 180 on Planetary Nebulae, ed. M. Peimbert, in press

Seaton, M. J., 1979, MNRAS, 187, 75P

Shaw, R. A., Dufour, R. J.,1995, PASP, 107, 896

Smits, D. P., 1996, MNRAS, 278, 683

Tylenda, R., Acker, A. Stenholm, B., 1993, Astron. Astrophys. Suppl., 102, 595

Vassiliadis, E., Wood, P.R., 1993, ApJ, 413, 641

Velázquez, H., White, S. D. M., 1995, MNRAS, 275, L23

Walsh, J. R., Roy, J.-R., 1993, MNRAS, 262, 27

Weideman, V., 1987, A&A, 188, 74

Webster, B. L., 1983, PASP, 95, 610

Whitelock, P. A., Irwin, M., Catchpole, R. M., 1996, New Astron, 1, 57

Wray, J. D., 1966, Thesis, Northwestern University

Zijlstra, A. A., van Hoof, P. A. M., Chapman, J. M., Loup, C., 1994, A&A, 290, 228

Zijlstra, A. A., Walsh, J. R., 1996, A&A, 312, L21

This 2-column preprint was prepared with the AAS LaTeX macros v4.0.